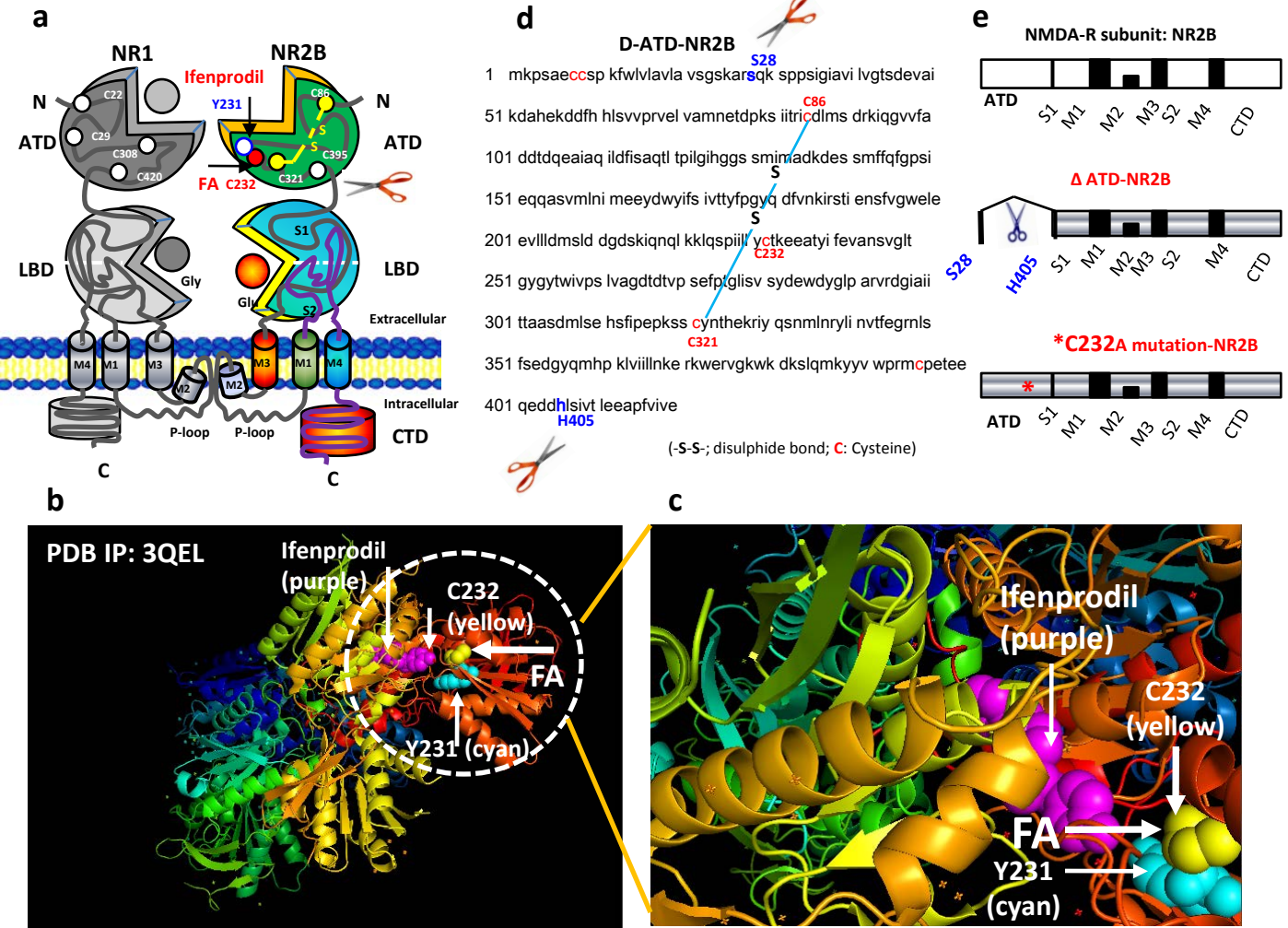
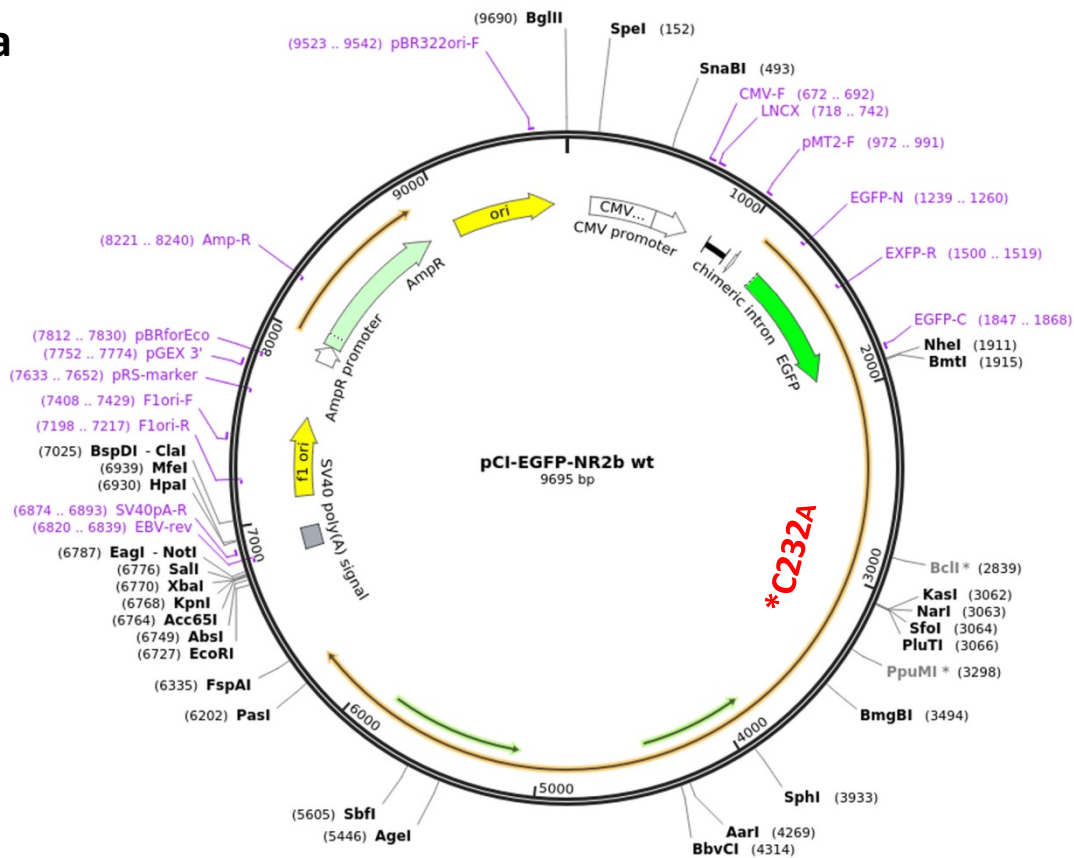
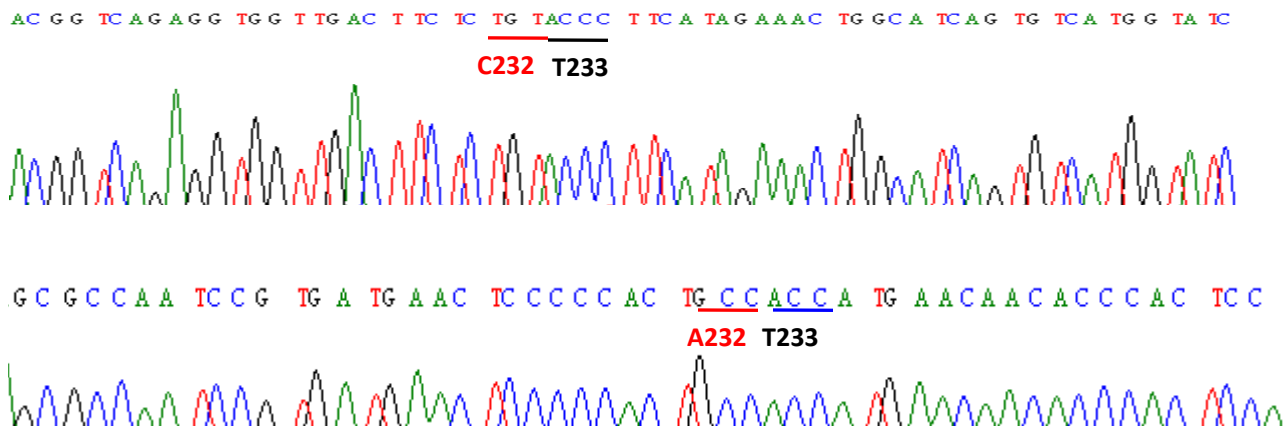


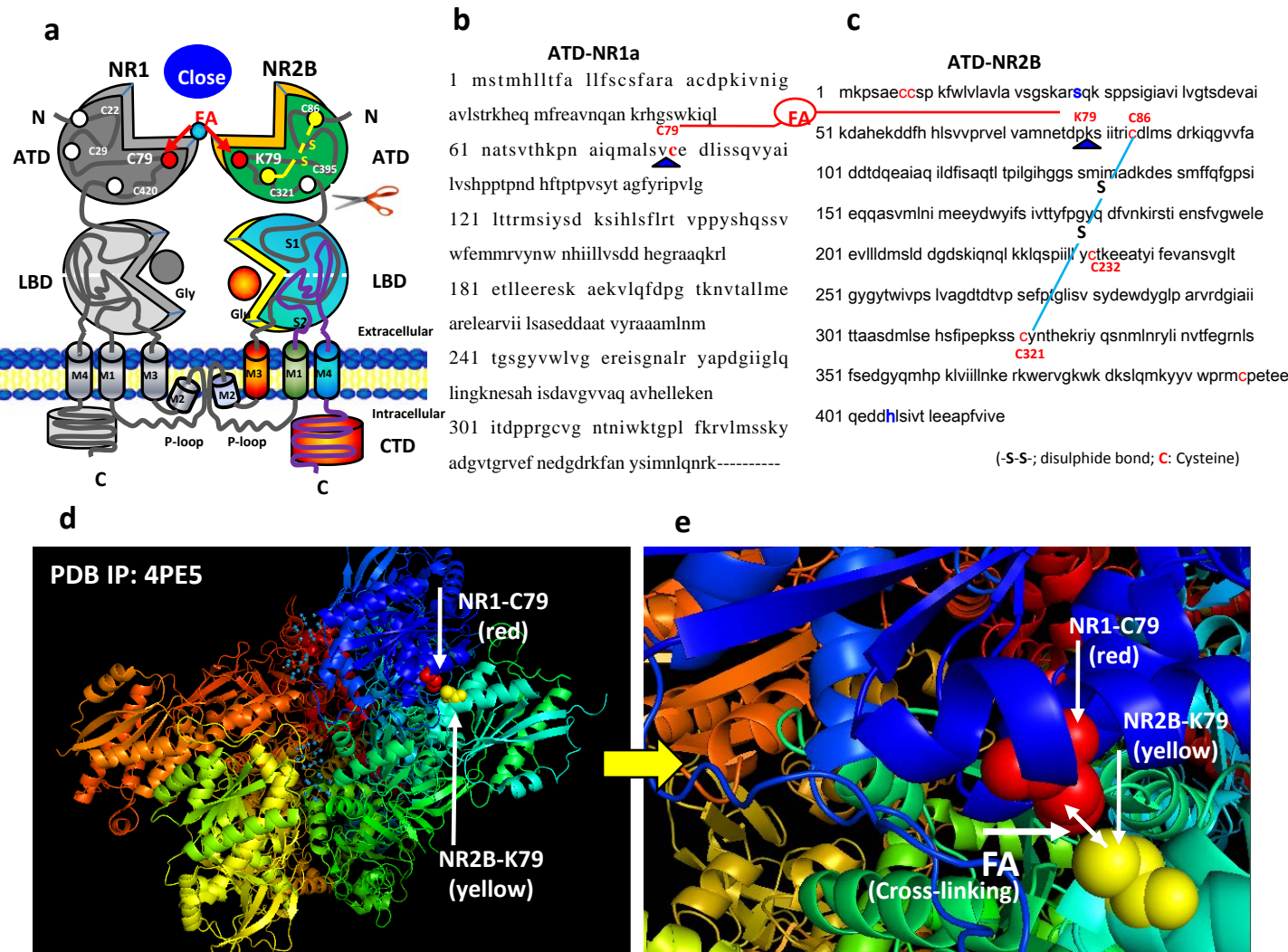
**Supplementary Figure 1. Formaldehyde (FA) at 0.05 mM enhances NMDA-induced intracellular  $\text{Ca}^{2+}$  influx in the cultured GFP-NR1/NR2B transfected CHO cells. (a)** The scheme for transfecting the plasmids of GFP-NR1/NR2B into CHO cells. **(b)** Intracellular  $\text{Ca}^{2+}$  influx measured using the probe Fluo-3 under laser scanning confocal microscopy. Ifen: Ifenprodil (an specific antagonist of NR2B).



**Supplementary Figure 2. A specific NR2B antagonist- Ifenprodil binds with Y231 and C232 residues to prevent the active FA connection with C232 site of N2B. (a)** The model of the complex of NR1 and NR2B. **(b)** The 3D crystal structure of Ifenprodil-binding with Y231 and C232 residues of NR1/NR2B (PDB IP: 3QEL). **(c)** The model of FA-binding with C232 of NR2B. **(d)** The sequences of deleting amino-terminal domain (D-ATD) of rat NR2B. **(e)** The model of deleting ATD of NR2B.

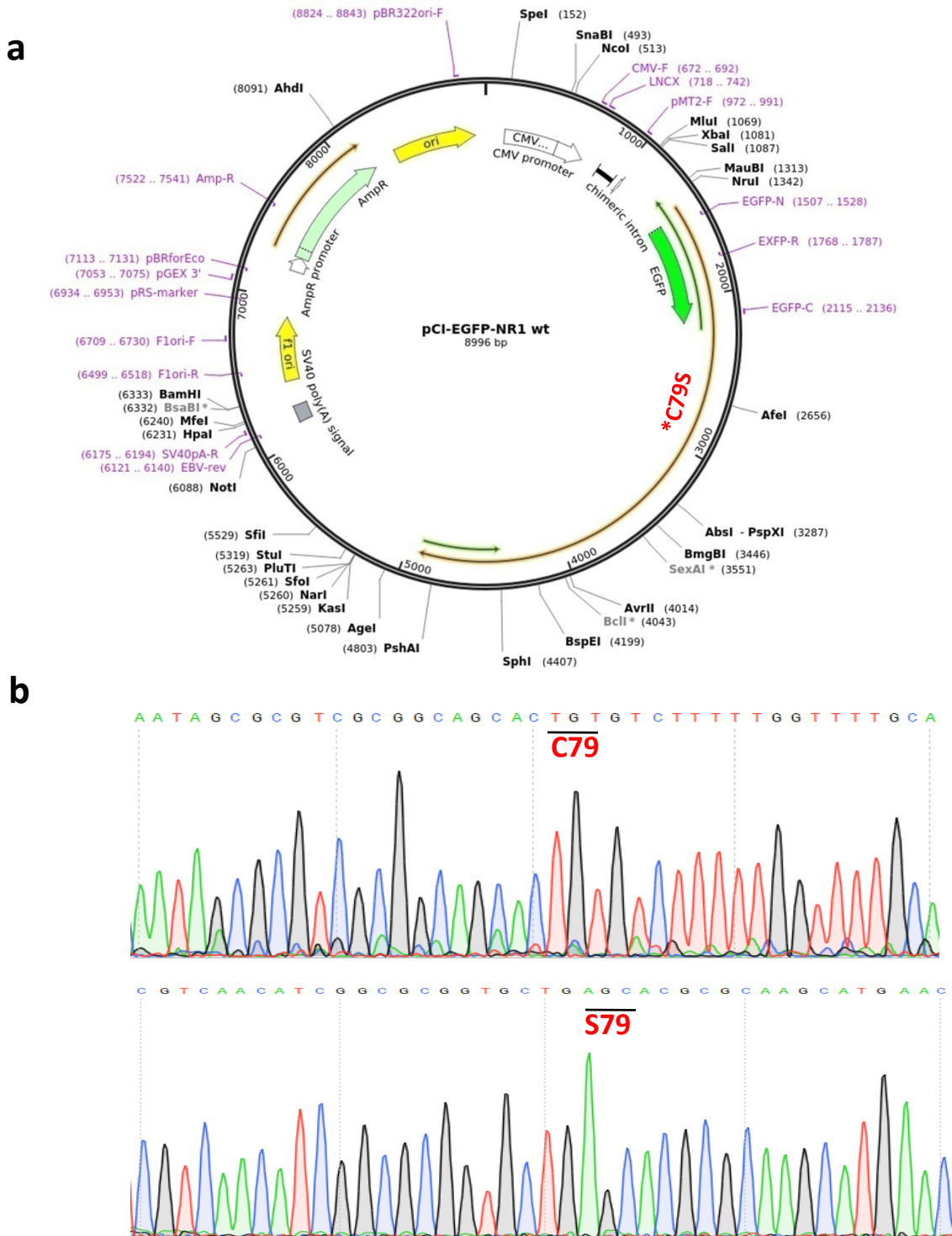
**a****b**

**Supplementary Figure 3. The identification of mutation in C232A site of NR2B of wild-type rat. (a) The plasmid of pci-EGFP-NR2B (9695 bp). (b) The DNA sequence of mutation in C232A (Cys codon: TGT; Ala codon: GCC) site of NR2B examined by gene sequencing.**

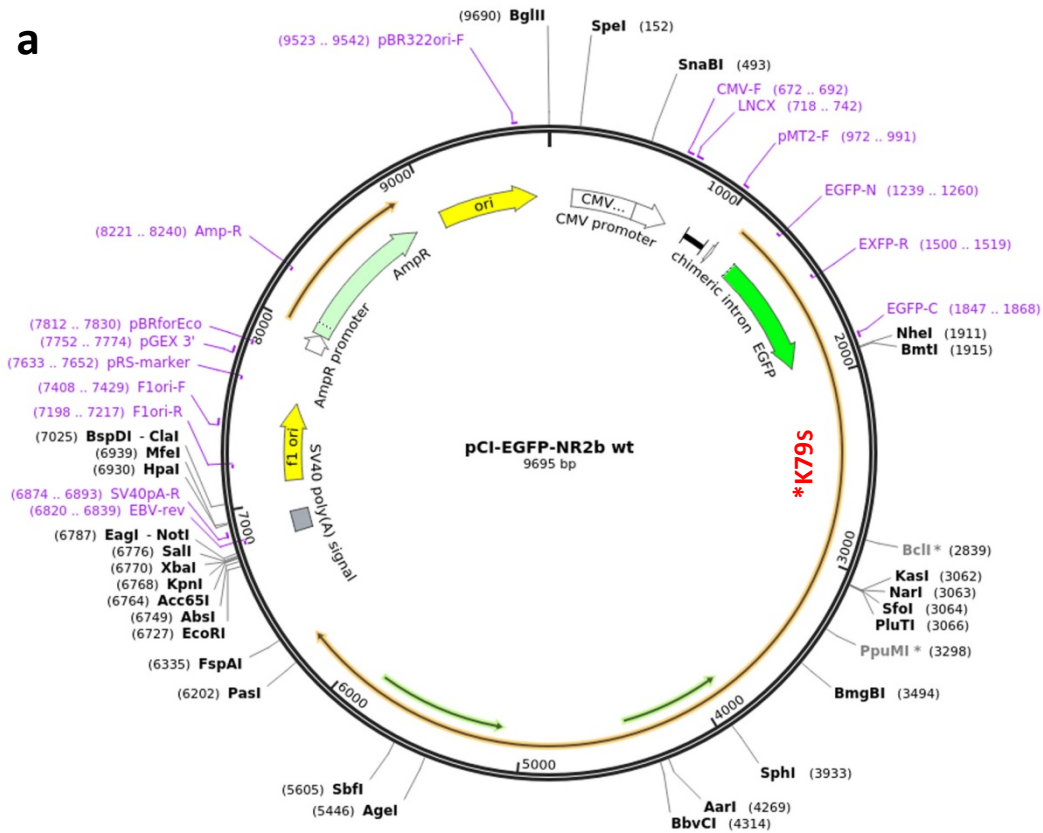
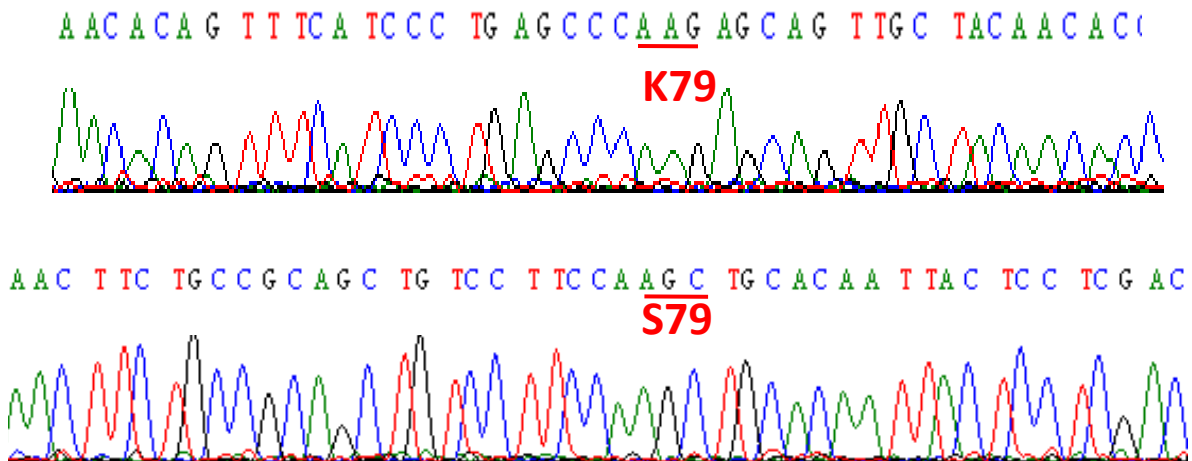


**Supplementary Figure 4. Excessive FA cross-links C79 residue of NR1 and K79 site of NR2B to block NMDA-receptor.** (a) The model of excessive FA-blocking the complex of NR1 and NR2B. (b, c) The sequences of amino-terminal domain (ATD) of rat NR1 and NR2B. (d) The 3D crystal structure of rat NR1/NR2B (PDB IP: 4PE5). (E) The model of excessive FA cross-linking C79 residue of NR1 and K79 site of NR2B.

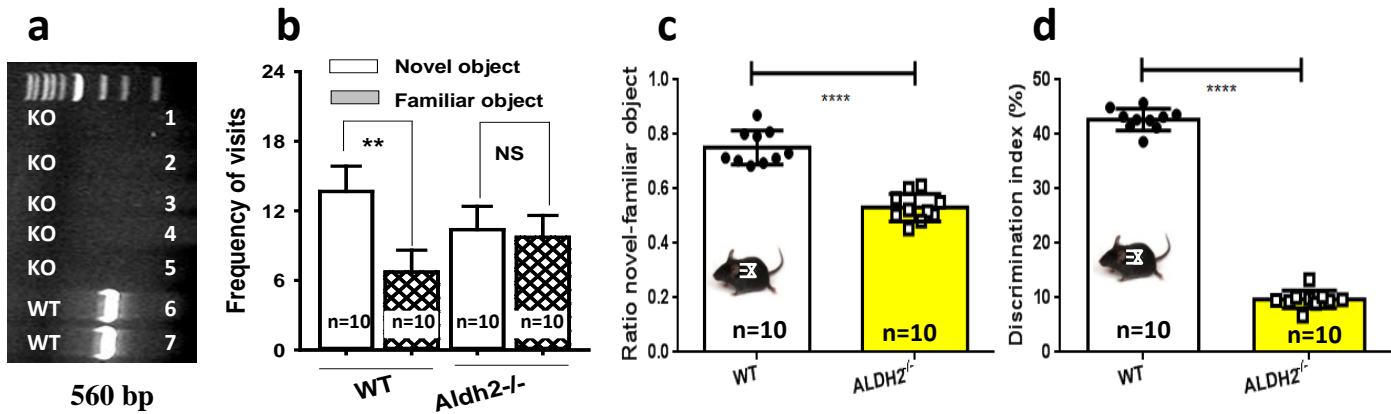




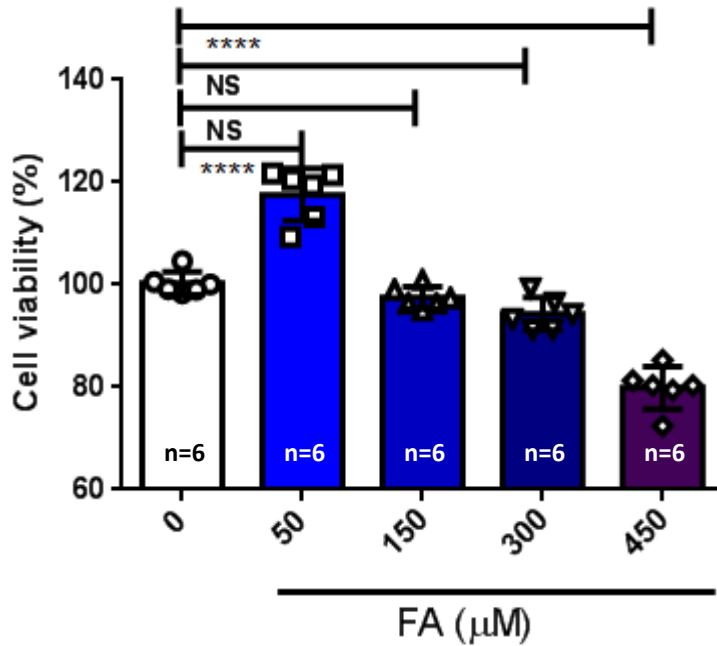
**Supplementary Figure 5. The identification of mutation in C79S site of NR1 of wild-type rat. (a) The plasmid of pci-EGFP-NR2B (8996 bp). (b) The DNA sequence of mutation in C79S (Cys codon: TGT; Ser codon: AGC) site of NR1 examined by gene sequencing.**

**a****b**

**Supplementary Figure 6. The identification of mutation in K79S site of NR2B of wild-type rat. (a)** The plasmid of pci-EGFP-NR2B (9695 bp). **(b)** The DNA sequence of mutation in K79S (Lys codon: AAG; Ser codon: AGC) site of NR2B examined by gene sequencing.

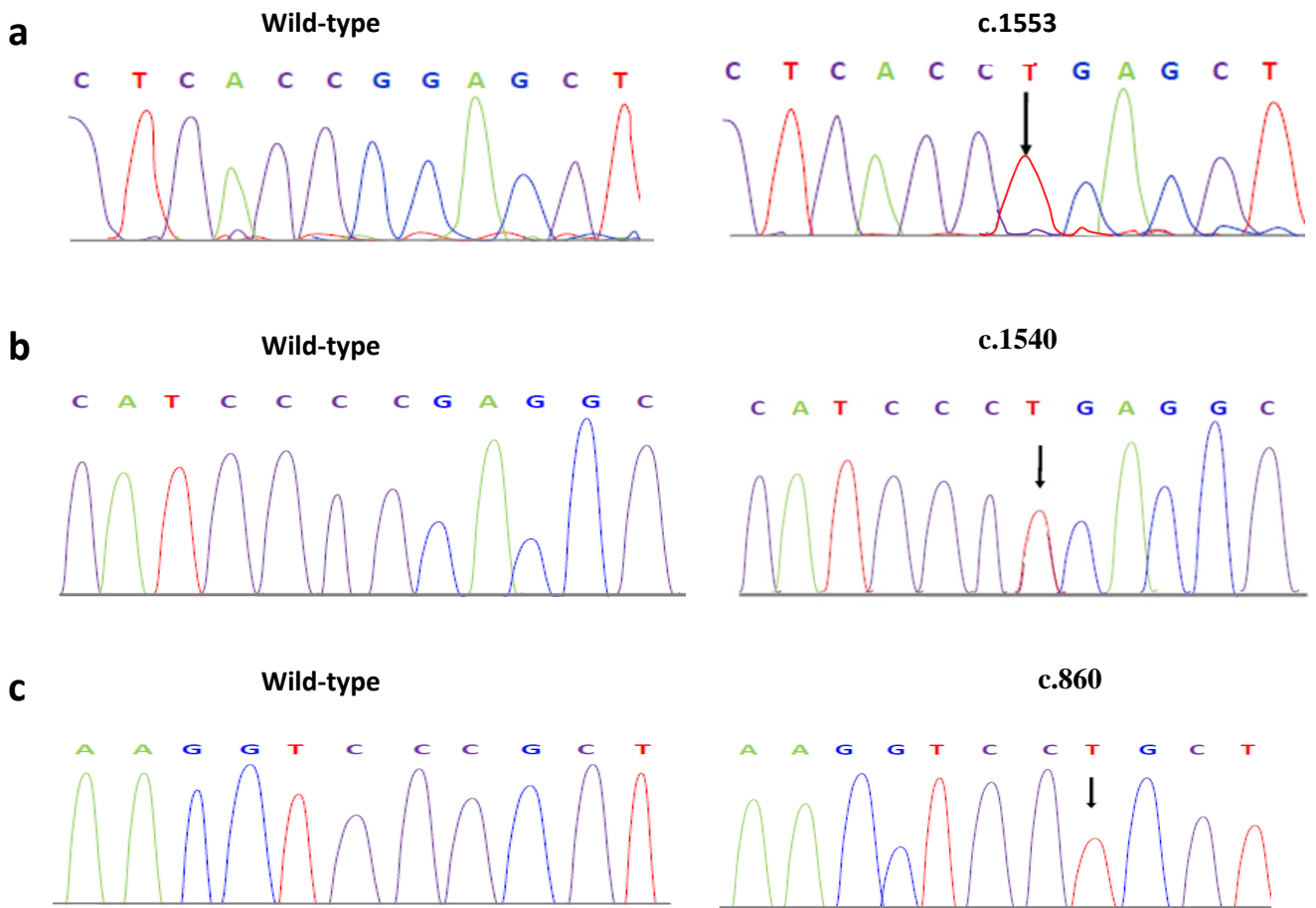


**Supplementary Figure 7. *Aldh2*<sup>-/-</sup> mice exhibit a marked decline in the novel object recognition task performance than wild-type mice.** (a) *Aldh2* gene in the mice was identified by PCR. (b) Frequency of visits to the novel and familiar objects for wild-type mice (WT) and *Aldh2*<sup>-/-</sup> mice. n = 10. (c) Ratio of time spent with the novel object in relation to the familiar object. (d) Discrimination index. The data are expressed as the mean ± standard deviation (s.e.m.). \*\**p* < 0.01. NS: no statistical significance.

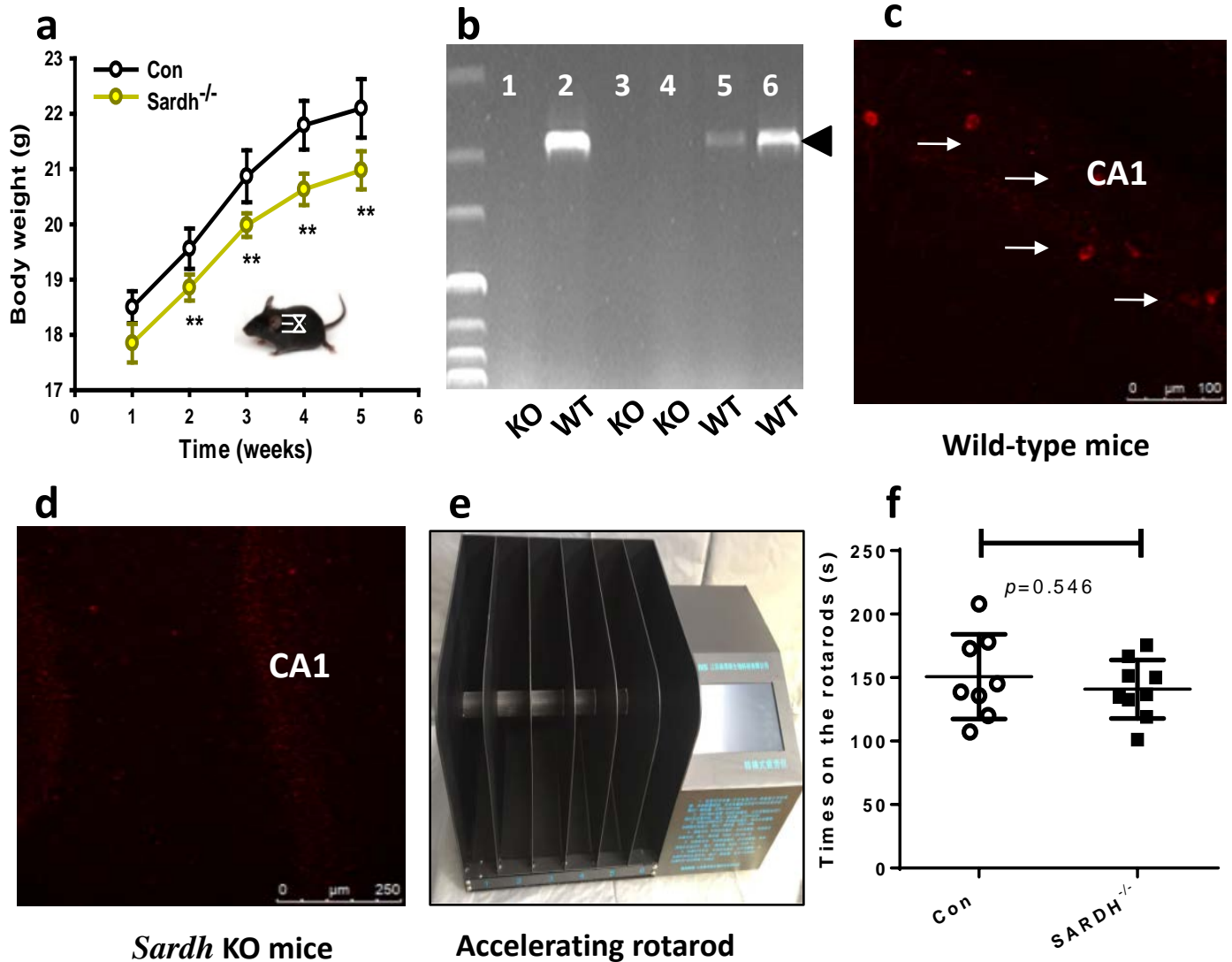


**Supplementary Figure 8. The effects of FA at different concentrations on cell viability in the cultured human SY5Y cells quantified by the Cell Counting Kit 8 (CCK-8).  $n = 6$  cultures per treatment. The data are expressed as the mean  $\pm$  standard deviation (s.e.m.). \*\* $p < 0.01$ . NS: no statistical significance.**

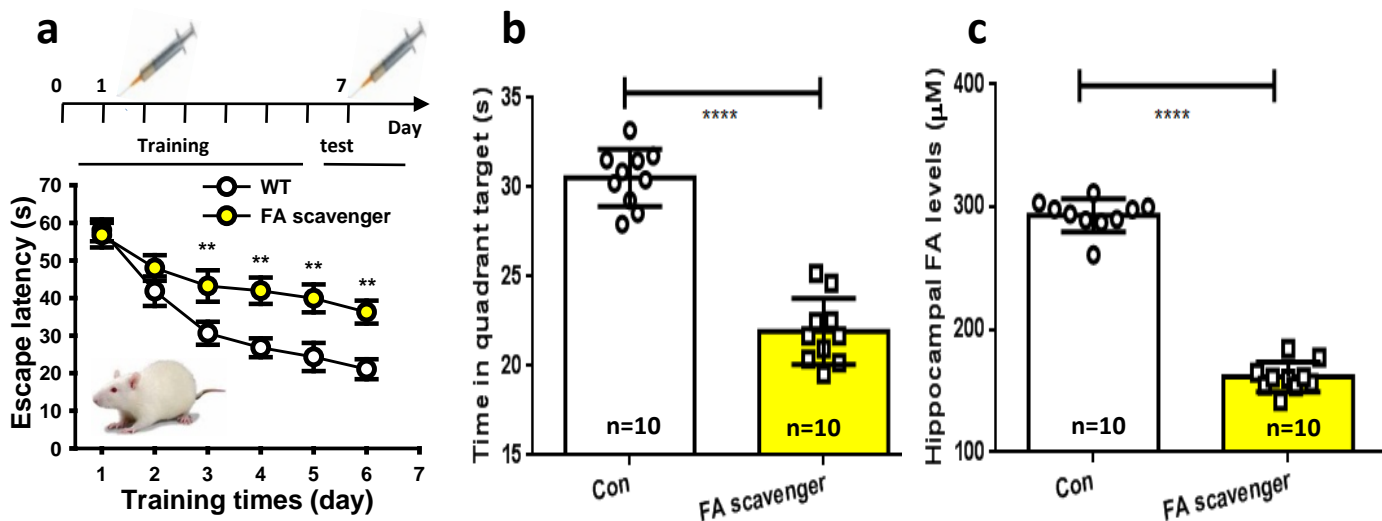




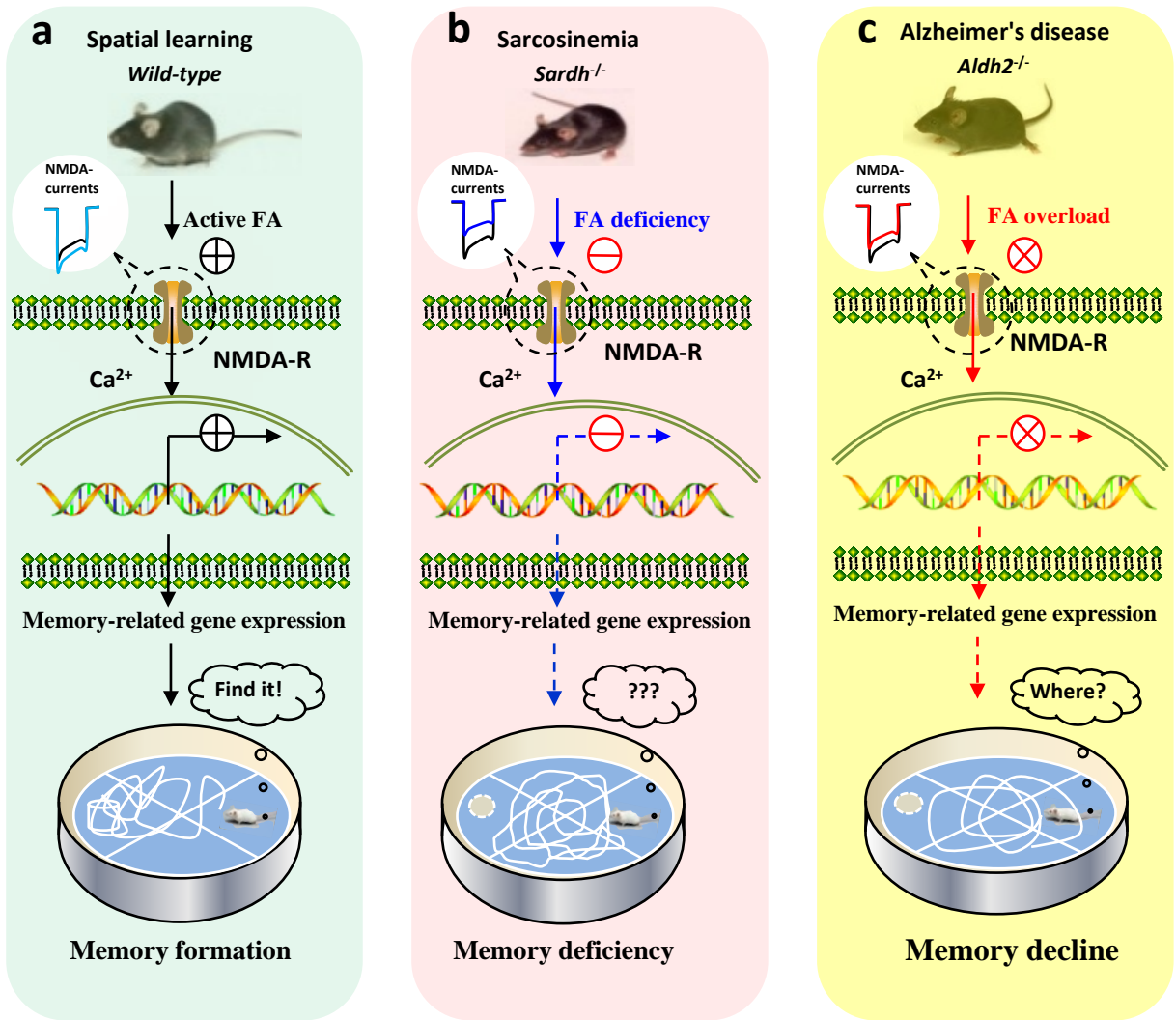
**Supplementary Figure 9. Sarcosinemia children (a rare neurodegenerative disease) with *SARDH* mutations at c.1553, c.1540, and c.860, respectively. The arrows indicate the site of the mutation.**



**Supplementary Figure 10. Knockout of *Sardh* affects body weight and SARDH expression in mice.** (a) Changes in body weight of *Sardh* KO mice and control mice from week 1 to 5. (b) *Sardh* gene in the mice was identified by PCR. (c, d) Low expression of SARDH proteins in the hippocampus of *Sardh*<sup>-/-</sup> mice than wild-type mice. (e, f) The motor abilities of *Sardh*<sup>-/-</sup> mice (n=9) than wild-type mice (n=8) examined by using accelerating rotarod (4 to 70 rpm, 5 minutes). Data are expressed as the mean  $\pm$  standard error (s.e.m.). \*\* $p < 0.01$ .



**Supplementary Figure 11. Formaldehyde deficiency by injecting of FA scavenger induces spatial memory deficits in healthy wild-type SD rats. (a)** Through the MWM test, *Post hoc* analyses of the mean escape latency values for the rats injected with FA scavenger ( $\text{NaHSO}_3$ ,  $300 \mu\text{M}$ ) were significant longer than control groups on day 3 ( $F_{(1,18)} = 2.18$ ,  $p = 0.005$ ), day 4 ( $F_{(1,18)} = 4.22$ ,  $p = 0.001$ ), day 5 ( $F_{(1,18)} = 5.87$ ,  $p = 0.003$ ) and day 6 ( $F_{(1,18)} = 5.19$ ,  $p = 0.004$ ). **(b)** Rats injected with FA scavenger had shorter time of staying in target quadrant.  $n = 10$ . **(c)** Hippocampal FA levels detected by Fluo-HPLC,  $n = 10$ . Data are expressed as the mean  $\pm$  standard error (s.e.m.).  $**p < 0.01$ .



**Supplementary Figure 12. Endogenous FA controls memory formation by regulating NMDA-R dually.** Briefly, spatial learning elicited a rapid generation of active FA in rat hippocampus; the concentrations attained were sufficient to facilitate NMDA-currents and enhanced memory formation. However, brain FA deficiency in sarcosinemia children associated with *SARDH* mutation or in *Sardh<sup>-/-</sup>* mice also led to cognitive deficits by reducing NMDA-currents. In addition, excess FA impaired memory in *aldh2<sup>-/-</sup>* mice and AD patients with *ALDH2* mutation by suppressing NMDA-R.

**Supplementary Table 1. Severe FA overload and cognitive decline in AD patients compared with healthy controls.**

Test items	Control (n = 87)	AD (n= 71)	P value
Age (Years old)	71.69 ± 2.75	73.52 ± 3.63	> 0.05
Sex (Man/Female)	25/25	23/22	> 0.05
Education (Years)	7.32 ± 2.78	7.09 ± 2.07	> 0.05
MMSE scores	27.68 ± 1.65	14.26 ± 2.09	< 0.01
Blood SA (μM)	22.14 ± 2.34	21.67 ± 1.78	> 0.05
Urine SA (μM)	14.84 ± 1.97	13.46 ± 2.46	> 0.05
Blood FA (μM)	75.45 ± 3.58	88.63 ± 3.45	< 0.01
Urine FA (μM)	23.32 ± 4.38	45.37 ± 5.38	< 0.01
ALDH2 activity (mOD/min)	2.36 ± 0.08	0.48 ± 0.05	< 0.01

SA: sarcosine; FA: formaldehyde; AD: Alzheimer's disease; MMSE: Mini-Mental State Examination

**Supplementary Table 2. Hardy-Weinberg equilibrium identified genotyping of *ALDH2* in AD patients and age-matched healthy controls.**

Groups	N	Genotypes			alleles	
		GG	GA	AA	G	A
AD ( n, %)	71	16 (22.53)	20 (28.16)	35 (49.29)	52 (36.61)	90 (63.38)
Con (n, %)	87	51 (58.62)	23 (26.43)	13 (14.94)	125 (71.83)	49 (28.16)
$\chi^2$	-	6.09	6.61	-	39.36	-
P value	-	0.014	0.01	-	< 0.0001	-
OR (95% CI)	-	0.36 (0.15-0.82)	0.32 (0.13-0.77)	-	4.41 (2.74-7.10)	-

OR: odd ratio; CI: confidential interval; “-”: No data; AD: Alzheimer's disease



**Supplementary Table 3. Severe FA deficiency and cognitive impairments in sarcosinemia children compared with healthy controls.**

<b>Test items</b>	<b>Control (n =31)</b>	<b>Sarcosinemia (n = 11)</b>	<b>P value</b>
Age (Years old)	6.08 ± 1.36	6.28 ± 2.03	> 0.05
Sex (Man/Female)	16/15	6/5	> 0.05
Weight (Kg)	20.79 ± 1.32	17.25 ± 1.15	< 0.01
WISC scores	103.35 ± 14.57	66.48 ± 9.69	< 0.01
Blood SA (μM)	21.05 ± 2.61	83.68 ± 3.55	< 0.01
Urine SA (μM)	13.47 ± 1.38	55.49 ± 2.52	< 0.01
Blood FA (μM)	82.05 ± 4.34	58.49 ± 2.81	< 0.01
Urine FA (μM)	30.26 ± 2.65	11.64 ± 1.79	< 0.01
SARDH activity (μM/min)	5.32 ± 0.64	1.38 ± 0.07	< 0.01

WISC: Wechsler Intelligence Scale for Children; SA: sarcosine; FA: formaldehyde